Effect of gallium doping on the characteristic properties of polycrystalline cadmium telluride thin film

OJO, A.A. and DHARMADASA, I <http://orcid.org/0000-0001-7988-669X>

EFFECT OF GALLIUM DOPING ON THE CHARACTERISTIC PROPERTIES OF POLYCRYSTALLINE CADMIUM TELLURIDE THIN FILM.

A. A. Ojo* and I. M. Dharmadasa

Electronic Materials and Sensors Group, Materials and Engineering Research Institute (MERI), Sheffield Hallam University, Sheffield S1 1WB, UK.

*Email: chartell2006@yahoo.com; Tel: +44 114 225 6910 Fax: +44 114 225 6930

ABSTRACT

Ga-doped CdTe polycrystalline thin films were successfully electrodeposited on glass/fluorine doped tin oxide (FTO) substrates from aqueous electrolytes containing cadmium nitrate ($Cd(NO_3)_2 \square 4H_2O$) and tellurium oxide (TeO_2). The effects of different Ga-doping concentrations on the CdTe:Ga coupled with different post-growth treatments were studied by analysing the structural, optical, morphological and electronic properties of the deposited layers using X-ray diffraction (XRD), ultraviolet-visible spectrophotometry, scanning electron microscopy, photoelectrochemical cell measurement and direct-current conductivity test respectively. XRD results show diminishing (111)C CdTe peak above 20 ppm Ga-doping and appearance of (301)M GaTe diffraction above 50 ppm Ga-doping indicating the formation of two phases; CdTe and GaTe . Although, reductions in the absorption edge slopes were observed above 20 ppm Ga-doping for the as-deposited CdTe:Ga layer, no obvious influence on the energy gap of CdTe films with Ga-doping were detected. Morphologically, reductions in grain size were observed at 50 ppm Ga-doping and above with high pinhole density within the layer. For the as-deposited CdTe:Ga layers, conduction type change from *n*- to *p*- were observed at 50 ppm, while the *n*-type conductivity were retained after post-growth treatment. Highest conductivity was observed at 20 ppm Ga-doping of CdTe. These results are systematically reported in this paper.

KEYWORDS: Electrodeposition, cadmium telluride, thin films, doping, gallium

1 INTRODUCTION

Based on electronic and optoelectronic properties, CdTe has proved to be an excellent II–VI semiconductor material with a near-ideal direct bandgap of 1.45 eV at ambient temperature for a single *p-n* junction. CdTe has attracted increasing interest due to its application in nuclear radiation detectors [1] and also in photovoltaic (PV) application. With photovoltaics (PV) being within the confines of this paper, CdTe-based solar cells have been well explored with its main deficiency being the formation of tellurium precipitates distributed randomly over the whole volume of the CdTe layer during growth [2–4]. The formation of Te precipitates within the CdTe layer creates uncertainty in the post-growth and/or post-growth treatment stoichiometry control. Post-growth treatment in the presence of Cd [5] and Cl [6] has been documented in the literature to reduce the Te precipitation [7]. Fernandez [2] has also demonstrated the possibility of eliminating Te precipitation from the bulk of CdTe layer using gallium melt treatment, although, high Te precipitation density were observable on the opposite side of the surface not in contact with the Ga melt treatment. This observation was described as the capability of Ga to dissolve the Te precipitates [2,5].

Although it has been argued that the complete elimination of Te precipitate in CdTe through growth modification or post-growth treatment conditions is impossible [2], this work focuses on the possibility of elimination of Te precipitates by the inclusion of Ga at different concentrations during the electrodeposition of CdTe. Furthermore, this work also evaluates the effect of Ga-doping on the electronic properties of CdTe to facilitate the device construction and thus promote their practical applications.

2 EXPERIMENTAL DETAILS

2.1 Electrolytic bath configuration and preparation

All the chemicals and substrates utilised in this work were procured from Sigma-Aldrich, United Kingdom. The two-electrode electroplating configuration utilised in the deposition of CdTe in this work comprises of highly conductive carbon rod as the anode, transparent conducting substrate glass/fluorine doped tin oxide (FTO) substrate as the cathode and an electrolytic bath containing appropriate precursor concentration. The electrodes are connected to a computerized GillAC potentiostat while been inserted into the electrolyte. 1200 nm CdTe was deposited from an aqueous electrolytic bath containing 1.5 M cadmium nitrate ($Cd(NO_3)_2$) with percentage purity of 99.997% and 0.0023 M tellurium dioxide (TeO_2) with percentage purity of 99.995%.

It should be noted that prior to the inclusion of TeO_2 in the electrolytic bath, 0.03 M of TeO_2 was dissolved by the addition of 30 ml concentrated nitric acid (HNO_3) due to its tendency of partly dissolving in acidic media [8]. The solution was stirred for 60 min to achieve full dissolution, afterwards, the TeO_2 solution was diluted by the addition of 400 ml deionised (DI) water. Only 5 ml of the TeO_2 were added to the CdTe electrolytic bath.

Afterwards, varied concentration from 0 ppm to 200 ppm of gallium sulphate ($Ga_2(SO_4)_3$) with a purity of 99.99% was added to all the CdTe baths containing same measured salts of Cd and Te precursors. The overall 300 ml aqueous solutions were contained in 500 ml polypropylene plastic beakers and housed in 1000 ml glass beakers. Low quantity of water is contained in the glass beaker to achieve uniformity in heating the electrolyte contained in the polypropylene beaker. The Ga-doped electrolytic baths were stirred for at least 5 h to achieve homogeneity before CdTe deposition. In addition, the pH, stirring rate and the electrolytic bath temperature were adjusted to 2.00±0.02, ~300 rpm and 85°C respectively prior to CdTe deposition.

All the CdTe layers were grown at an optimal cathodic voltage of 1400 mV based on optical, morphological, compositional and structural analysis as reported in one of the previous publications [9] from similar precursors.

2.2 Substrate preparation and treatments

Prior to the deposition of the semiconductor layers on the glass/FTO conducting substrates, the glass/FTO layers were cleaned in an ultrasonic bath containing soap solution and rinsed in running DI water. Afterwards, the substrates were degreased using the acetone and methanol and rinsed in deionised water afterwards [10]. The glass/FTO substrates were transferred directly into the deposition electrolyte immediately after rinsing in DI water. It should be noted that the glass/FTO substrates utilised in this sets of experiments were TEC7 with sheet resistance 7 Ω/sq. The glass/FTO sheets were cut into 3.0×3.0 cm^2 with an active area 2.5×3.0 cm^2 in contact with the electrolyte.

After CdTe growth from different Ga-doped CdTe baths, the glass/FTO/CdTe layer was cut into three with each having an active area 1×2.5 cm^2. One of the layers is left as-deposited, while the other two were dipped into an aqueous solution containing 0.1M $CdCl_2$ and 0.1M $CdCl_2$ plus 0.05M $Ga_2(SO_4)_3$ respectively at room temperature. The layers were left to air-dry and heat-treated at 420°C for 20 min in air to improve both their material and electronic properties [2,11]. In this work, the as-deposited, $CdCl_2$ treated and $CdCl_2$+ $Ga_2(SO_4)_3$ treated CdTe layers will be referred to as AD, CCT and GCT respectively. All the glass/FTO/CdTe:Ga layers were analytically explored to ascertain the effect of in-situ Ga inclusion in CdTe and the effect of the post-growth treatments.

2.3 Experimental techniques used

Information on lattice parameters and sample texture such as crystallite size, preferred orientation and phase identification of electroplated CdTe layers were obtained using Philips PW 3,710 X'pert diffractometer with Cu-Kα monochromator of wavelength λ = 1.54 Å. For this sets of experiments, the X-ray generator tension and current were respectively adjusted to 40 kV and 40 mA. Studies on the optical properties of the grown CdTe layers were performed at room temperature within the wavelength range of 200–1000 nm using Cary 50 Scan ultraviolet-visible (UV–Vis) spectrophotometer. Prior to absorption measurements, the baseline was set using blank glass/FTO to eliminate the effect of glass/FTO absorption. Information on both the morphological properties of the electroplated CdTe layers was obtained using FEI Nova 200 NanoSEM at a magnification of ×60,000. To determine the conductivity type of the grown CdTe layers, photoelectrochemical (PEC) cell measurement was performed. This was performed by dipping the glass/FTO/CdTe layer into an aqueous electrolyte containing 0.1 M sodium thiosulphate ($Na_2S_2O_3$) to form a solid/liquid junction. The difference between the measured voltages under illuminated (V_L) and dark (V_D) conditions at constant time duration gives the electrical conductivity type of the layer and the magnitude of the signal indicates the suitability of doping concentration of the semiconducting layer for fabricating electronic devices [12]. The direct current (DC) conductivity measurement was performed to determine the electrical conductivity of the CdTe:Ga layers using Rera solution fully automated I–V measurement system.

3 RESULTS AND DISCUSSION

3.1 Structural analysis

The structural analysis was performed to determine the optimal Ga-doping concentration in CdTe bath. This can be determined by observing the highest peak intensity, crystallinity, and

crystallite size. Figure 1 (a - c) shows the X-ray diffraction (XRD) measured between 2θ=20° and 2θ=70° for CdTe layers doped with Ga between 0 ppm and 200 ppm under AD, CCT and GCT conditions. While Figure 1 (d) shows the cubic (111) CdTe XRD diffraction intensity of CdTe grown from CdTe bath containing different concentrations of Ga-doping ranging from 0 ppm to 200 ppm. Asides from the XRD diffraction associated with glass/FTO at ~26.64°, ~33.77°, ~37.85°, ~51.64° and ~65.62° 2θ angle, CdTe peaks associated with (111) cubic, (220) cubic and (311) cubic were observed at 2θ≈23.95°, 2θ≈38.60° and 2θ≈45.80° respectively. From observation, the most intense diffraction, which signifies the preferred orientation of CdTe growth was observed at 2θ≈23.95° for all the post-growth treatment conditions explored in this work. Similarly, a gradual increase in the diffraction intensity was observed with increasing Ga-doping from 0 ppm to 20 ppm as shown in Figure 1 (a-d). This observation can be associated with an increase in crystallinity of CdTe along the (111)C plane due to the reduction and dissolution of Te precipitation [2] and the incorporation of Ga as a substitutional dopant. An increase in the doping of Ga above 20 ppm results into a reduction in diffraction intensity of the CdTe (111)C and a total collapse of the peak at 200 ppm Ga-doping and above. Subsequently, an emergence of GaTe diffraction peak was observable above 20 ppm Ga-doping under all the explored condition explored in this work. Furthermore, an increase in the GaTe peak intensity at 2θ≈27.23° was noticeable with increasing Ga concentration. It should be noted that the reduction of CdTe (111)C diffraction intensity above 20 ppm Ga-doping in CdTe bath can be attributed to competing crystalline phases of CdTe and GaTe. Furthermore, this observation emphasises the replacement of Cd atoms with Ga atoms in the crystal lattice to form GaTe [5]. Only two valence electrons out of three available for bonding of Ga atoms were utilised in the formation of bonds with neighboring Te atoms while the excess electron is donated to the lattice to aid the *n*-type conduction.

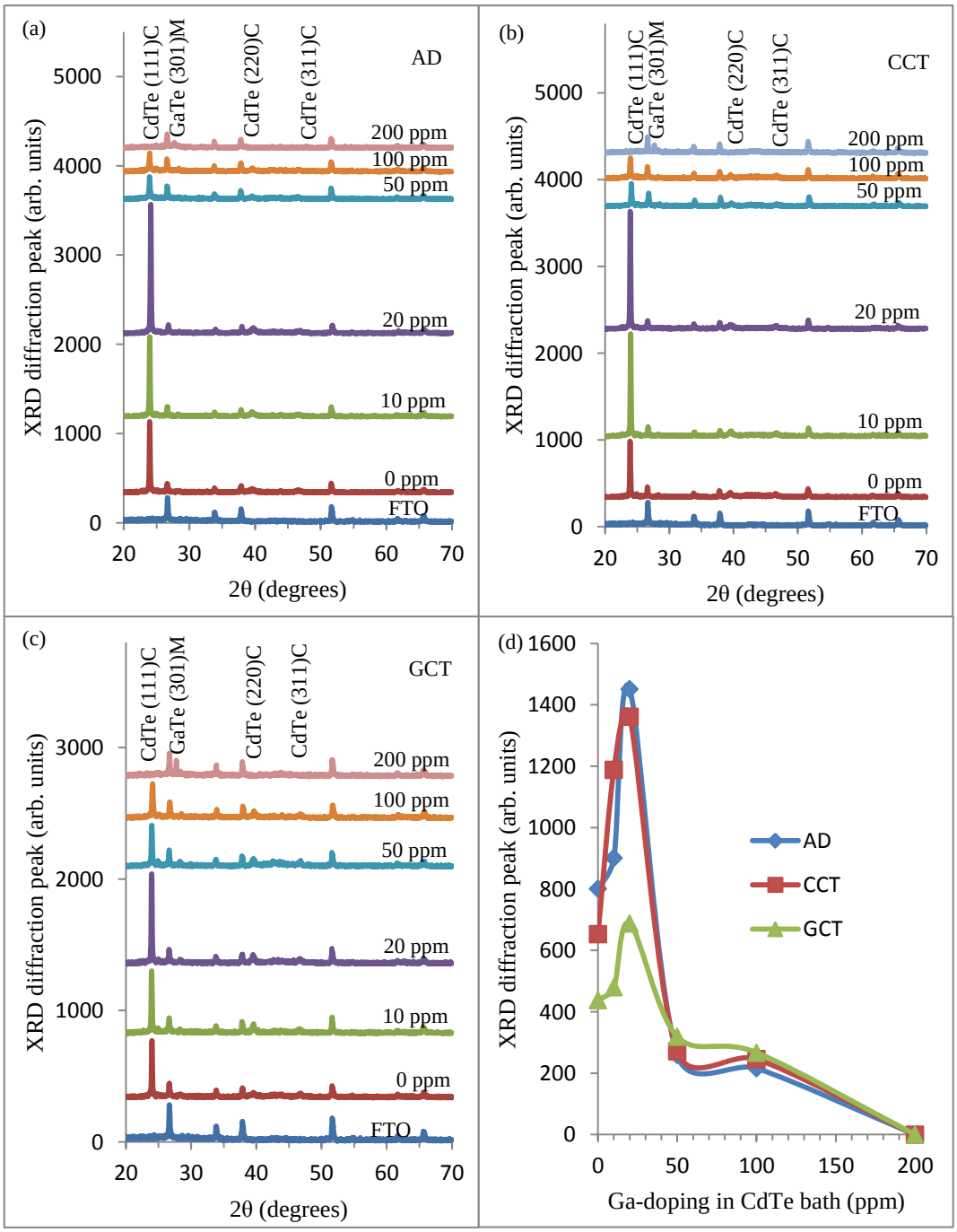

Figure 1: Typical XRD patterns of CdTe at different galium doping concentrations for (a) AD (b) CCT and (c) GCT-CdTe layers. (d) is the typical plot of CdTe:Ga (111) cubic peak intensity against Ga-doping of CdTe baths.

The extracted XRD data in this work match the Joint Committee on Powder Diffraction Standards (JCPDS) reference file number 01-075-2086-cubic for CdTe and 01-075-2220-

monoclinic for GaTe. Table 1 shows the XRD analysis of CdTe layers grown at different gallium concentrations. While the crystallite sizes (*D*) of each of the CdTe layers at different Ga-doping was calculated using Scherrer formula as shown in Equation (1) where θ is the Bragg angle, β is the full-width-at-half-maximum (FWHM) of the diffraction intensity in radian and λ is the wavelength of the X-rays used (1.54 Å).

$$D = \frac{0.94\lambda}{\beta \cos\theta} \tag{1}$$

Uniformity in both the FWHM and crystallite size was observed for the entire as-deposited CdTe layers as shown in Table 1. After CCT treatment of the CdTe layers, reduction in FWHM to 0.129° and resulting increase in crystallite sizes to 65.3 nm were observed for CdTe layers doped with Ga within the range of 0 ppm and 20 ppm. Subsequently, reductions in the crystallite size were observed for CdTe layers doped with Ga at 50 ppm and above. This observation is due to the reduction of crystallinity due to the formation of two phases; CdTe and GaTe. The replacement of Cd atom which has an atomic radius of 1.61 Å with Ga atoms which has a comparatively lower atomic radius of 1.36 Å may lead to contraction of the crystal lattice [10,13]. The same phenomenon was observed with the GCT treated CdTe:Ga layers.

Table 1: XRD analysis of CdTe layers grown at different Ga-doping concentrations

AS-DEPOSITED

Doping (ppm)	2θ (°)	d-spacing (Å)	FWHM (°)	Crystallite size (nm)
0	23.95	3.712	0.162	52.3
10	23.95	3.712	0.162	52.3
20	24.12	3.688	0.162	52.3
50	23.94	3.714	0.162	52.3
100	23.95	3.712	0.162	52.3

$CdCl_2$ TREATED

Doping (ppm)	2θ (°)	d-spacing (Å)	FWHM (°)	Crystallite size (nm)
0	24.10	3.689	0.130	65.3
10	23.95	3.713	0.130	65.3
20	23.90	3.720	0.130	65.3
50	23.98	3.708	0.162	52.3
100	23.93	3.716	0.162	52.3

$CdCl_2$+ $Ga_2(SO_4)_3$ TREATED

Doping (ppm)	2θ (°)	d-spacing (Å)	FWHM (°)	Crystallite size (nm)
0	23.94	3.714	0.130	65.3
10	23.99	3.707	0.162	52.3
20	23.94	3.714	0.162	52.3
50	23.96	3.710	0.162	52.3
100	24.08	3.693	0.195	43.6

Furthermore, it is appropriate to look at the stability of the two compounds; CdTe and GaTe at this stage. The stability of inorganic compounds is given by its heat of formation or the enthalpy value (ΔH) given by Equation (2) and (3).

$$\text{(reactant)}\ Cd + Te \rightarrow CdTe\ \text{(product)} + \Delta H \tag{2}$$

$$\text{(reactant)}\ Ga + Te \rightarrow GaTe\ \text{(product)} + \Delta H \tag{3}$$

The product with the largest negative value of ΔH is more stable according to [14]. As depicted in Figure 2, the ΔH values of CdTe and GaTe are -50.6 $kJmol^{-1}$ and -62.6 $kJmol^{-1}$ [15-16] respectively as reported in the literature. These values indicate that GaTe is more stable and therefore as the Ga concentration increases beyond 20 ppm, GaTe compound formation takes place within the layer. The presence of these two competing phases allows the deterioration of crystallinity and the complete collapse of the (111)C peak originating from *CdTe.*

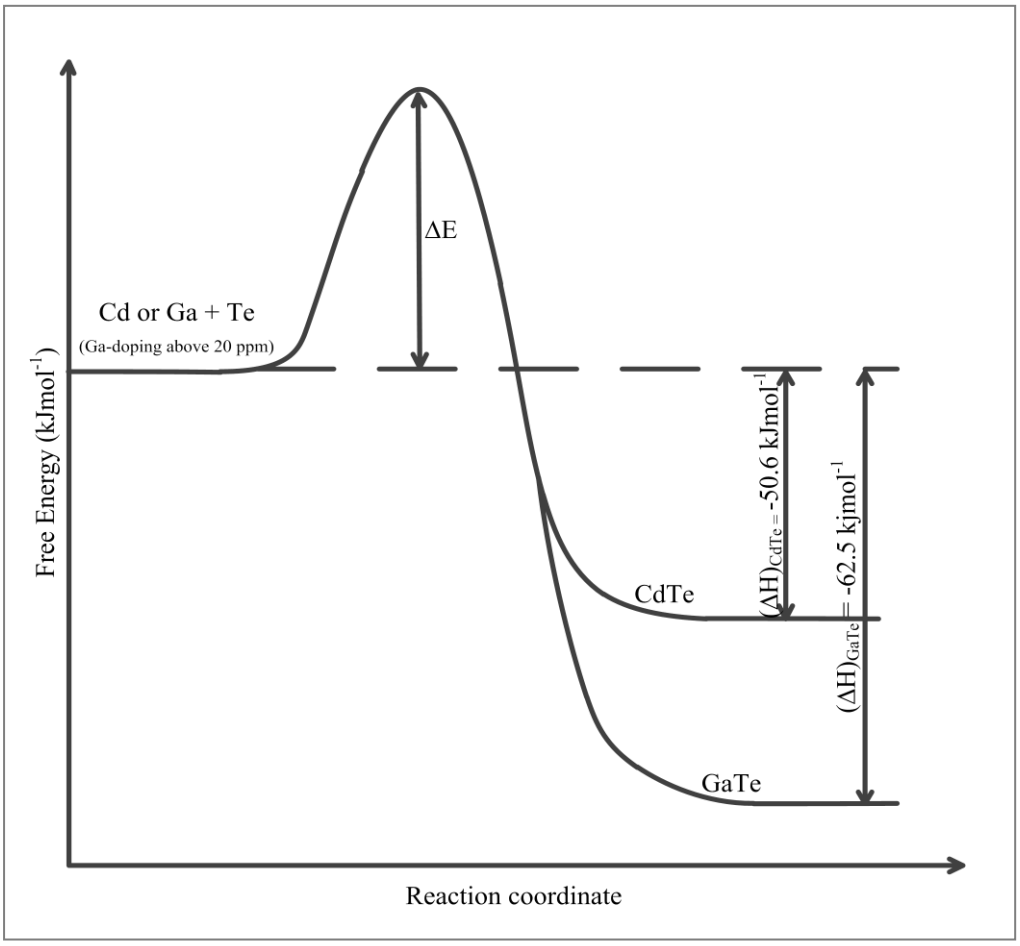

Figure 2: Free energy graph depicting the enthalpy ΔH_f at 298 K for both CdTe and GaTe compounds.

3.2 Optical properties analysis

Figure 3 (a - c) shows the optical absorption of CdTe:Ga layers under AD, CCT and GCT conditions respectively, while Figure 3 (d) shows the graph of absorption edge slope against Ga-doping concentration in CdTe bath. It should be noted that due to the removal of the effect of glass/FTO as explained in Section 2.3, only the absorption of the CdTe:Ga is captured. As observed in Figure 3 (a - c), the optical bandgaps of the entire deposited CdTe layer at varying Ga-doping concentration were within the range of 1.48±0.02 eV. This observation shows the dominance of CdTe even with the incorporation of Ga and formation of GaTe as observed in Section 3.1. Alteration in the absorption edges of CdTe:Ga layers with varying Ga-doping concentration were also observed as shown in Figure 3 (d). The steepest absorption edge slope which signifies the best quality of semiconductor layer [17] were observed at Ga-doping of 20 ppm, 20 ppm and 0 ppm under AD, CCT and GCT conditions respectively (Figure 3d). As reported in the literature, increase in steepness of the semiconductor materials absorption edge signifies lesser defects and impurity energy levels in the thin film [18]. Furthermore, sharp absorption edge also allows more photons to be absorbed even at low CdTe thickness of few microns [17]. This optical result therefore shows the possibility of having better solar cell efficiency using 20 ppm gallium doped CdTe:Ga. This observation indicates an initial improvement in the material quality for CdTe:Ga layers with Ga-doping of 0 ppm to 20 ppm under AD and CCT conditions as shown in Figure 3 (d) and also suggest CdTe:Ga material quality saturation at 20 ppm Ga-doping under the conditions explored in this set of experiments. An increase in Ga-doping above 20 ppm for CdTe:Ga layers under AD and CCT shows the detrimental effect to the CdTe:Ga material quality as the reduction in the absorption edge slope suggest for Ga-doping of 50 ppm and above. This observation is in accord with the structural analysis as explored in Section 3.1.

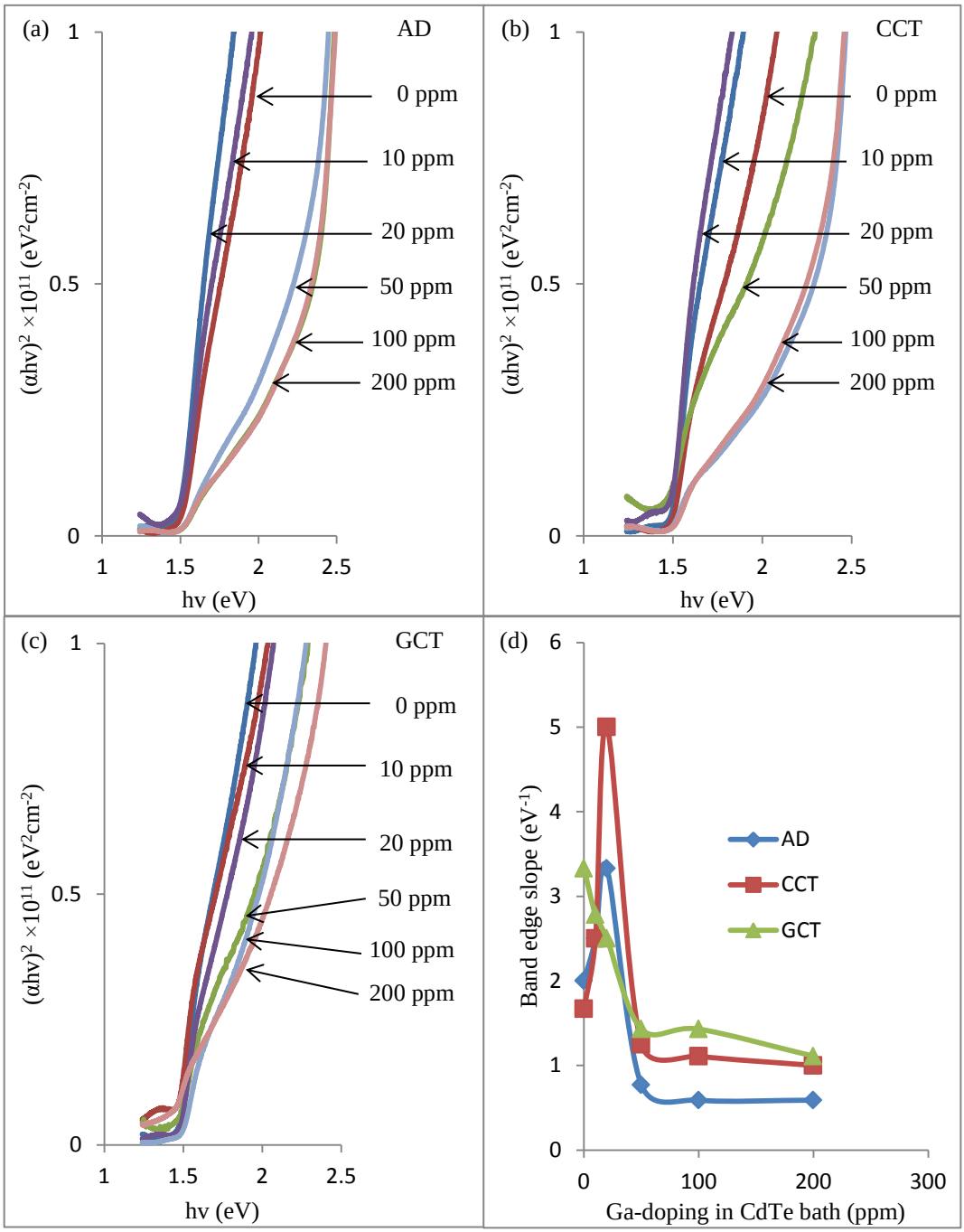

Figure 3: Optical absorption of CdTe:Ga with different doping concentrations of gallium under (a) AD, (b) CCT and (c) GCT conditions, while (d) is the absorption edge slope of CdTe:Ga under AD, CCT and GCT conditions against Ga-doping concentration.

Furthermore, a dissimilar trend of absorption edge slope for the GCT treated CdTe:Ga layers was observed with as-grown layers doped with 0 ppm giving the highest absorption edge slope. Although, it is well known that the treatment of CdTe in the presence of Ga melt improves the material properties of CdTe by dissolving Te precipitates [2,5], the

incorporation of superfluous Ga into the CdTe lattice results into detrimental effect such as the formation of competing phases of CdTe and GaTe as observed in Section 3.1. It should be noted that the effect of persistent photoconductivity and photoinduced persistent absorption associated with Ga-doped CdTe at 77 K [19] were not observed due to the room temperature in which the experiments were performed.

3.3 Morphological analysis

Figure 4 (a - l) show the scanning electron microscope (SEM) micrographs of CdTe layers grown from an electrolytic bath containing 0, 20, 50 and 100 ppm Ga-doping under AD, CCT and GCT conditions. From observation, the initial incorporation of Ga-doping from 0 to 20 ppm under AD condition shows agglomeration of grains and full coverage of the underlying glass/FTO substrate. At 50 ppm Ga-doping, a reduction in grain and agglomeration sizes were observed, while, no clear grain boundaries were observed at 100 ppm and above. The deterioration in grain and agglomeration sizes can be attributed to competing crystalline phases of CdTe and GaTe. As expected, improvement after CCT and GCT post-growth treatment was observed with larger grain size at 0 to 20 ppm. The treatment of CdTe doped with Ga higher than 20 ppm shows detrimental effect such as comparatively smaller grains and high pinhole density. It should be noted that the pinholes observed in the 0 to 20 ppm Ga CdTe layers might be due to optimisation requirement for both heat treatment temperature and duration, Ostwald ripening, the thickness of the CdTe layer utilised and the utilisation of glass/FTO substrate as it is well known that CdTe grows better on smooth semiconductor (with CdS being a preferred partner) surfaces due to its columnar growth configuration. Based on this observation, it could be said that the superfluous incorporation of Ga through in-situ Ga-doping of CdTe or GCT is detrimental to CdTe layer property. This observation is in accord with the structural and optical analyses discussed in Sections 3.1 and 3.2. It should

be noted that the crystallite size as calculated using XRD does not correspond to the grain size as seen on the SEM micrograph but the grains are formed from several crystallites.

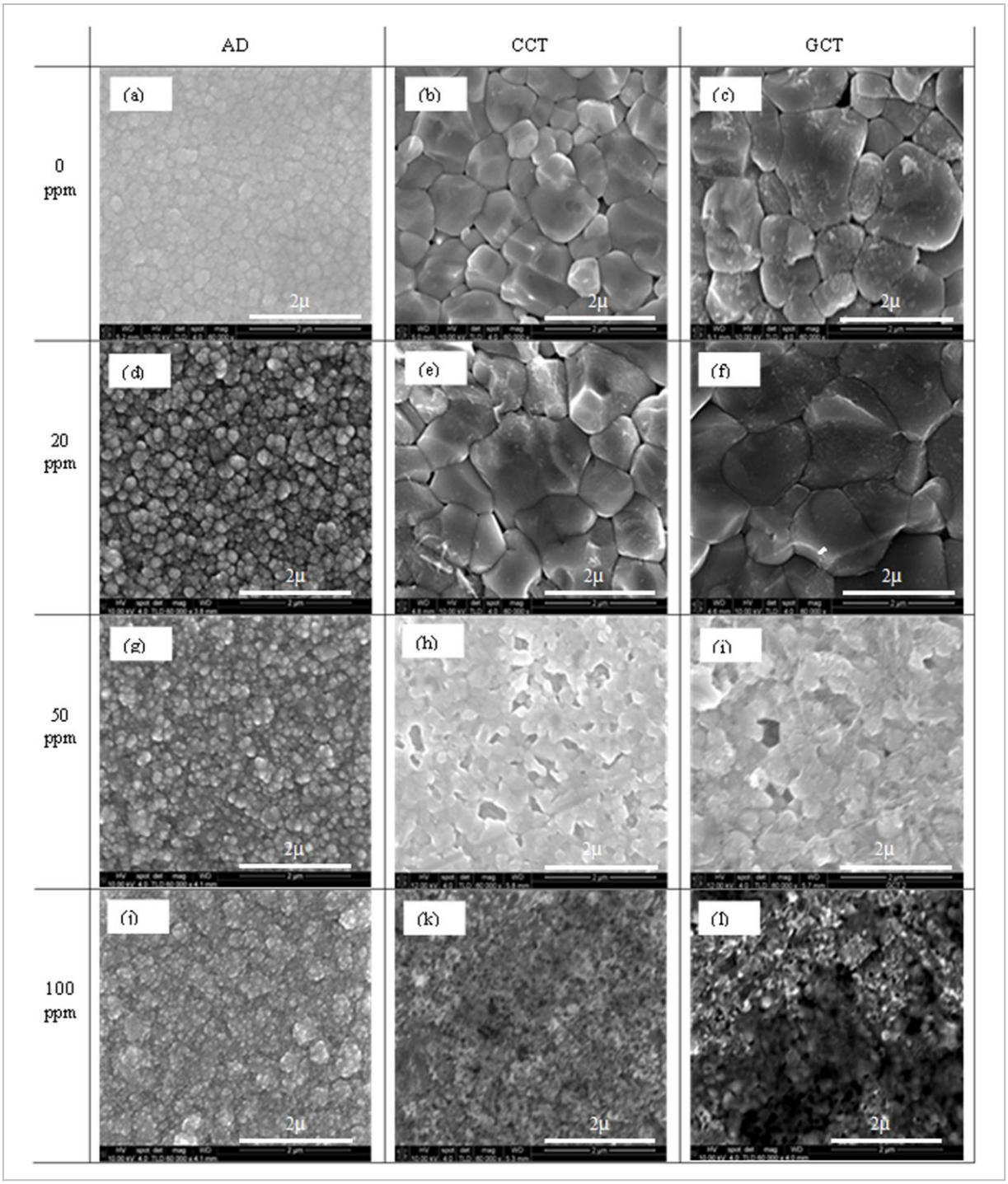

Figure 4: SEM micrographs for CdTe;Ga layers grown with Ga-doping concentrations between 0 and 100 ppm which have undergone AD, CCT and GCT treatments.

3.4 Electronic property analysis

3.4.1 Photoelectrochemical (PEC) cell measurement

Figure 5 shows the photoelectrochemical cell measurement against Ga-doping concentration in CdTe bath. The CdTe layers utilised for these experiments were grown at 1400 mV. For the as-deposited CdTe:Ga layers, a retention of the *n*-type conductivity was maintained from 0 to 20 ppm, while a transition from *n*- to *p*- type was observed at 50 ppm and above. The transition from *n*- to *p*- type conductivity might be due to the excess replacement of Cd with Ga, whereby the doping effect is converted into an alloying effect with the complete alteration of the crystallite lattice and compound.

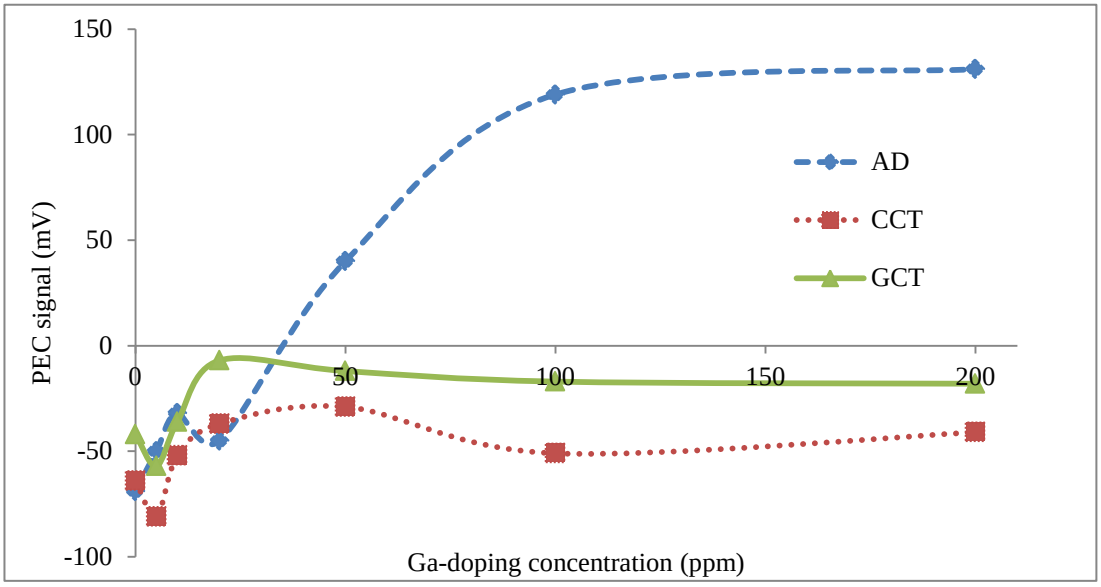

Figure 5: Photoelectrochemical cell measurements for AD,CCT and GCT treated Ga-doped CdTe thin films.

The excess incorporation of Ga at 50 ppm and above might either create an acceptor like defects which might be more dominant than the *n*-doping characteristics of Ga in CdTe. Furthermore, the formation of GaTe which is typically *p*-type semiconductor material [20-21] as observed in Section 3.1 might also be the possible cause. After both CCT and GCT, the conductivity type of CdTe:Ga at all doping concentrations explored show an *n*-type electrical conductivity due to the changes occurring in the CdTe:Ga layers. This might be through the

sublimation of excess element and the removal of acceptor-like dopants during heat treatment. This conductivity type change after heat treatment indicates that the *n*-doping is dominant rather than any *p*-like native defects.

3.4.2 DC conductivity properties analysis

Figure 6 (a - b) show the graph of both the resistance and conductivity against Ga-doping concentration of CdTe after CCT and GCT post-growth treatment conditions. For this experiment, ~1.5 µm thick CdTe:Ga grown from CdTe baths with varied Ga concentration from (0 – 100) ppm were utilised. The glass/FTO/CdTe:Ga layers were cut into two and each half were either treated with CCT or GCT. 2 mm diameter indium ohmic contacts with a thickness of ~100 nm were evaporated on the treated CdTe:Ga layers. It should be noted that only the CCT, and the GCT post-growth treated CdTe:Ga were explored due to its significance in the determination of device properties.

The electrical resistance (*R*) of the structure was calculated from the Ohmic I-V data obtained under dark condition using Rera Solution PV simulation system using the glass/FTO/CdTe:Ga/In and glass/FTO as contacts. While the resistivity values were obtained using Equation (4).where ρ, *R*, *A*, and *L* are the resistivity, resistance, contact area and film thickness respectively.

$$\rho = \frac{RA}{L} \tag{4}$$

The comparable trend in the CCT and the GCT treated CdTe:Ga layers were observed as shown in Figure 6. The incorporation of Ga-doping from 0 ppm shows a gradual increment in conductivity which can be attributed to the excess electron donated from the replacement of Cd atoms with Ga atoms in the crystal lattice [5]. A possible solubility limit of CdTe:Ga was

observed at ~20 ppm Ga-doping due to the gradual reduction in the conductivity [22] in all conditions observed. Furthermore, the domination of *p*-type conductivity over the *n*-CdTe as discussed in Section 3.4.1 due to the superfluous incorporation of Ga-incorporation above 20 ppm might also be a determining factor as it is well known that the mobility and the conductivity of *p*-type semiconductors are lower than that of its *n*-type counterpart [23].

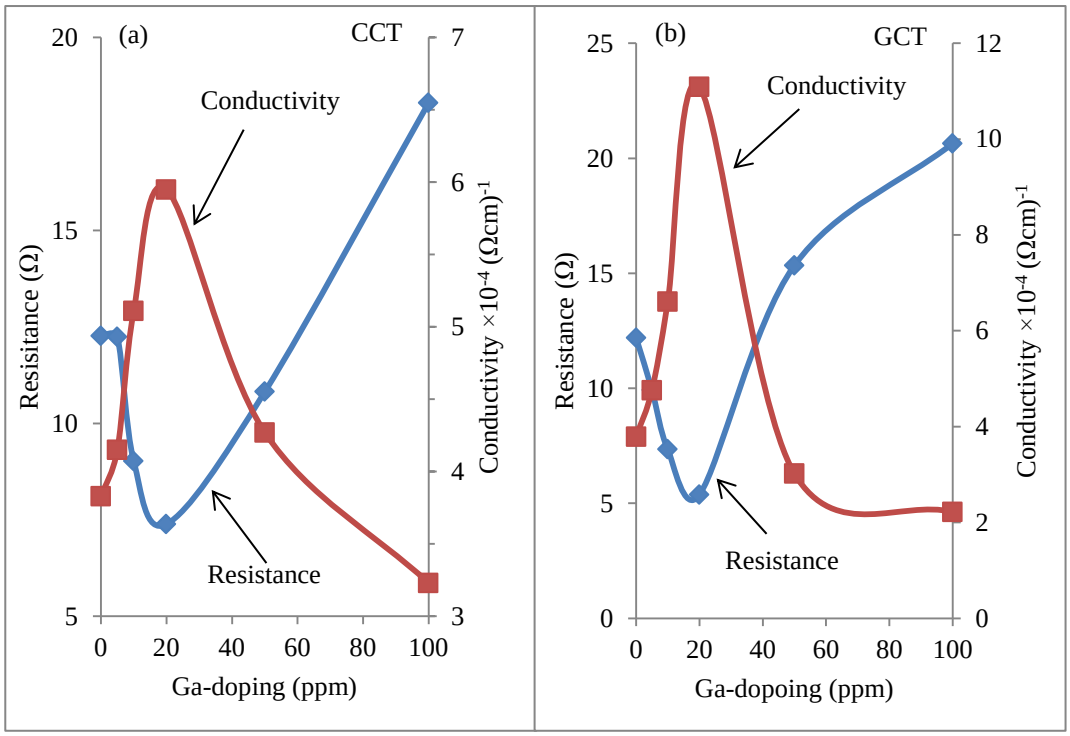

Figure 6: Electrical resistance and conductivity plotted against Ga-doping concentration in the CdTe bath after (a) CCT and (b) GCT treatments.

4 CONCLUSION

The work presented in this paper has successfully explored the effect of in-situ Ga-doping concentration in CdTe electrolytic bath and the inclusion of Ga in the regular $CdCl_2$ post-growth treatment on electrodeposited CdTe layers. The XRD results show increase in the preferred (111) cubic CdTe peak from 0 to 20 ppm Ga-doping for all the post-growth treatment explored. While a gradual reduction in the (111) cubic CdTe peak was observed with an emergence of (301) monoclinic GaTe peak at 50 ppm Ga-doping and above, coupled

with a reduction in crystallite size. The optical analysis shows improvement in absorption edge with in-situ Ga-doping of CdTe bath from 0 to 20 ppm. Morphologically, a comparative reduction in the grain size was observed at high in-situ Ga-doping at 50 ppm and above. PEC cell measurement shows a transition of conductivity type from *n*-type to *p*-type at high Ga-doping of 50 ppm and above for the as-deposited CdTe layers. Work is progressing to utilise the unique properties observed in structural, optical, morphological and electrical conduction type analysis in these layers in solar cell device structures.

ACKNOWLEDGEMENT

The contributions made by H.I. Salim, O.I. Olusola and M.L. Madugu are acknowledged by the authors. The principal author would also like to thank the Tertiary Education Fund (TETFund) Nigeria, Sheffield Hallam University, and Ekiti State University, Ado-Ekiti, Nigeria, for their support to undertake this research.

DECLARATION OF INTEREST

We have no conflicting interest.

REFERENCES

1. T. L. Chu, S. S. Chu, Y. Pauleau, K. Murthy, E. D. Stokes, and P. E. Russell, J. Appl. Phys. **54**, 398 (1983).

2. P. Fernández, J. Optoelectron. Adv. Mater. **5**, 369 (2003).

3. K. Zanio, *Semiconductors and Semimetals* (Academic Press, New York, 1978).

4. K. Peters, A. Wenzel, and P. Rudolph, Cryst. Res. Technol. **25**, 1107 (1990).

5. N. V. V Sochinskii, V. N. N. Babentsov, N. I. I. Tarbaev, M. D. Serrano, and E. Dieguez, Mater. Res. Bull. **28**, 1061 (1993).

6. H. N. Jayatirtha, D. O. Henderson, a. Burger, and M. P. Volz, Appl. Phys. Lett. **62**, 573 (1993).

7. I. M. Dharmadasa, O. K. Echendu, F. Fauzi, N. A. Abdul-Manaf, O. I. Olusola, H. I. Salim, M. L. Madugu, and A. A. Ojo, J. Mater. Sci. Mater. Electron. (2016).

8. C. G. Morris, *Academic Press Dictionary of Science and Technology* (Academic Press, San Diego, 1991).

9. H. I. Salim, V. Patel, a. Abbas, J. M. Walls, and I. M. Dharmadasa, J. Mater. Sci. Mater. Electron. **26**, 3119 (2015).

10. A. A. Ojo and I. M. Dharmadasa, J. Electron. Mater. **45**, 5728 (2016).

11. I. M. Dharmadasa, Coatings **4**, 282 (2014).

12. N. B. Chaure, A. P. Samantilleke, R. P. Burton, J. Young, and I. M. Dharmadasa, Thin Solid Films **472**, 212 (2005).

13. L. Jin, Y. Linyu, J. Jikang, Z. Hua, and S. Yanfei, J. Semicond. **30**, 112003 (2009).

14. M. A. Cengel, Y. A. and Boles, *Thermodynamics: An Engineering Approach*, 5th ed. (McGraw-Hill, 2006).

15. V. P. Vasil'ev, Inorg. Mater. **43**, 115 (2007).

16. O. Chang-Seok, L. D. Nyung, and C. Oh, Calphad **16**, 317 (1992).

17. A. Bosio, N. Romeo, S. Mazzamuto, and V. Canevari, Prog. Cryst. Growth Charact. Mater. **52**, 247 (2006).

18. J. Han, C. Spanheimer, G. Haindl, G. Fu, V. Krishnakumar, J. Schaffner, C. Fan, K. Zhao, a. Klein, and W. Jaegermann, Sol. Energy Mater. Sol. Cells **95**, 816 (2011).

19. E. PŁaczek-Popko, Z. Gumienny, J. Trzmiel, and J. Szatkowski, Opt. Appl. **38**, 559 (2008).

20. K. C. Mandal, R. M. Krishna, T. C. Hayes, P. G. Muzykov, S. Das, T. S. Sudarshan, and S. Ma, IEEE Trans. Nucl. Sci. **58**, 1981 (2011).

21. A. M. Mancini, C. Manfredotti, A. Rizzo, and G. Micocci, J. Cryst. Growth **21**, 187 (1974).

22. E. Elangovan and K. Ramamurthi, Thin Solid Films **476**, 231 (2005).

23. P. J. Sellin, A. W. Dazvies, A. Lohstroh, M. E. Özsan, and J. Parkin, IEEE Trans. Nucl. Sci. **52**, 3074 (2005).

LIST OF FIGURES